

# Numerical Investigation of Damage Types Through Concrete Dam by Multi-Laminate Model upon Instrumentation Data

**Seyaed Amirodin Sadrnejad**

**Department of Civil Engineering, K. N. Toosi University of Technology  
P. O. Bax15875-4416, Tehran, Iran**

Email: sadrnejad@kntu.ac.ir

## **Abstract**

In maintenance of concrete made dam, damages and their type's outcome internally after strong earthquake are generally judged upon engineering experience and guess which mostly may be not logical and even not true. A meso-scale multi-laminate based damage model has been developed and employed to simulate the location, orientation and type of internal damages due to any change at boundaries such as earthquake. The proposed model can rationally describe the semi-macroscopic behavior of quasi-brittle materials, and especially concrete, under the effects of any change sensed by overall instrumentation data outcome with regards to the pre-existing values before damage. The capability of proposed model was investigated through modeling the interaction of meso-scale heterogeneities and formulating the damage constitutive law governing on predefined sampling planes interactions. Accordingly, any compressive/tensile/shearing on plane conditions created upon experimental tests (under both quasi-static and dynamic conditions) can be numerically simulated. The analysis will include discussion of failure/post failure pattern as well as fragment distribution. The capability of proposed model in crack progression and fragmentation is investigated through the analysis of any plain and reinforced concrete dam to show the ideal damages across dam body.

**Keywords:** instrumentation data analysis, internal damage, crack type, damage orientation.

## **1. INTRODUCTION**

Concrete infrastructures such as dam require regular control by instrument data acquisition and assessment to ensure safety for maintenance practice. These assessments effort can verify and confirm in place, position and geometry of any internal damages such as crack propagation or crack extended continuity which may decrease strength and increase seepage through vein. The proposed Model has been developed upon multi-laminate framework which defines the small continuum structural units as an assemblage of particles and voids that fill infinite spaces between the sampling planes. This model has appropriately justified material particles and voids interactions as the contribution of interconnection forces in overall macro-mechanics internal deformation mechanism. Upon these assumptions, nonlinear deformations are to occur due to sliding, separation/closing of the boundaries and elastic deformations are the overall responses of structural unit bodies. Therefore, the overall deformation of any small part of the medium is composed of total elastic response and an appropriate summation of sliding, widening/closing phenomenon under the current effective normal and shear stress/strains on predefined random sampling planes. Representation of the overall stress/strain/compliance tensor in terms of semi-micro or micro level stresses and the condition, number and magnitude of contact forces has long been the aim of numerous researchers (Christofferson, et. al., (1981) [1], Nemat-Nasser, et. al., (1983) [2]. The multi-laminate developed by Sadrnejad, et al., (1992, 2017) [3, 4], is capable of predicting the behaviour of geo-materials, such as rock/concrete, on the basis of sliding mechanisms, elastic behaviour of intact parts and possibilities to see different plasticity models for the most possible sliding orientations. To overcome limitations exceeding continuum mechanic limits, certain calibration parameters can be obtained with regards to the concrete type and a linear isotropic medium with no remaining porosity is assumed by means of polyhedron bodies [5,6]. The artificial polyhedrons are assumed in between 17 sliding planes, passing through each point in medium. The location of tip heads of normal to the planes defining corresponding direction cosines are shown on the surface of unit radius sphere. In ideal case, the normal integration is considered as summing up the individual micro effects correspond to infinite number of micro sampling planes [7].

## 2. MULTI-LAMINATE CONCEPT

A multi-laminate model incorporating a mixture of the kinematic and static constraints should be physically more realistic than simply is supported by continuum mechanics law. Figure 1 shows Real aggregation of particles and 2D representation of artificial polyhedron. Figure 2 shows the geometry and orientation of 17 sampling planes tangent on sphere surface and in cubes. The values of weighted coefficients of 17 independent planes are shown in Table 1.



Figure 1 (a) Real aggregation of particles; (b) 2D representation of aggregation of artificial polyhedron

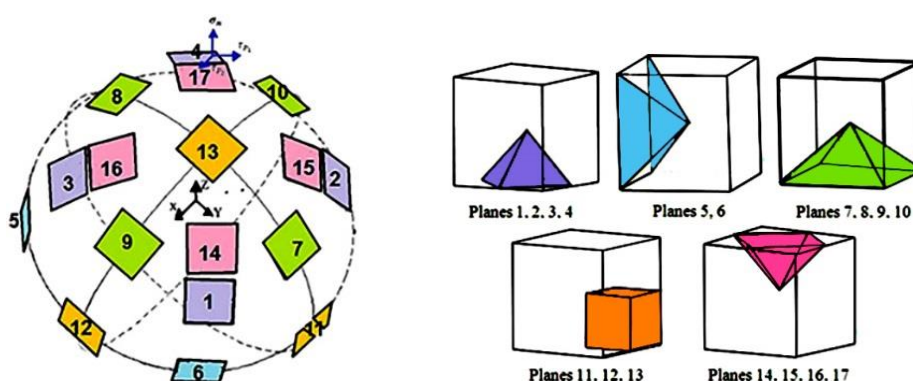


Figure 2 direction of 17 sampling planes on the surface of sphere and in cubes

Table 1: direction cosines and weighted coefficients for 17 planes

Plane No	normal axis			$w_i$
	$n_1$	$n_2$	$n_3$	
1	$\frac{\sqrt{3}}{3}$	$\frac{\sqrt{3}}{3}$	$\frac{\sqrt{3}}{3}$	.020277985
2	$\frac{\sqrt{3}}{3}$	$-\frac{\sqrt{3}}{3}$	$\frac{\sqrt{3}}{3}$	.020277985
3	$-\frac{\sqrt{3}}{3}$	$\frac{\sqrt{3}}{3}$	$\frac{\sqrt{3}}{3}$	.020277985
4	$-\frac{\sqrt{3}}{3}$	$-\frac{\sqrt{3}}{3}$	$\frac{\sqrt{3}}{3}$	.020277985
5	$\frac{\sqrt{2}}{2}$	$\frac{\sqrt{2}}{2}$	0	.058130468
6	$-\frac{\sqrt{2}}{2}$	$\frac{\sqrt{2}}{2}$	0	.058130468
7	$\frac{\sqrt{2}}{2}$	0	$\frac{\sqrt{2}}{2}$	.030091134
8	$-\frac{\sqrt{2}}{2}$	0	$\frac{\sqrt{2}}{2}$	.030091134
9	0	$-\frac{\sqrt{2}}{2}$	$\frac{\sqrt{2}}{2}$	.030091134
10	0	$\frac{\sqrt{2}}{2}$	$\frac{\sqrt{2}}{2}$	.030091134
11	1	0	0	.038296881
12	0	1	0	.038296881
13	0	0	1	.029390060
14	$\frac{\sqrt{6}}{6}$	$\frac{\sqrt{6}}{6}$	$\frac{\sqrt{2}}{\sqrt{3}}$	.019070616
15	$\frac{\sqrt{6}}{6}$	$-\frac{\sqrt{6}}{6}$	$\frac{\sqrt{2}}{\sqrt{3}}$	.019070616
16	$-\frac{\sqrt{6}}{6}$	$\frac{\sqrt{6}}{6}$	$\frac{\sqrt{2}}{\sqrt{3}}$	.019070616
17	$-\frac{\sqrt{6}}{6}$	$-\frac{\sqrt{6}}{6}$	$\frac{\sqrt{2}}{\sqrt{3}}$	.019070616

The spaces between 17 sliding planes, passing through each point in medium divide three dimension domains in several polyhedrons. The choice of 17 planes for the solution of any three dimensional problems is a fair number that can comply compatibility condition as well as equilibrium through the use of numerical integration.

Any set of six or nine strain components apply to  $dx dy dz$  element sides can be transferred to a new coordinate built on a sampling plane where, one coordinate axis is normal to plane surface. According the use of 17 planes in multi-laminate numerical integration (sadnejad, (2017)) [4], the strain tensor at any point with 6 or 9 components is equal to numerically integrated weighted 17 on plane, 3 components strain tensor.

Consequentially, gradual application of abnormal differences of instrument recorded values converted to equivalent stress/strain increments and solving to satisfy minimum energy level on any of  $dx dy dz$  element leads to carry out internal sampling plane deformations which can introduce damaged widened/slides on plane cracks. This analytical method is to be used to detect internal damages through concrete dam body.

### 3. PORE PRESSURE AND DEFORMATION EFFECTS

Under an externally applied stress, quick acceleration, deformation or crack progressions are forced into more intimate concrete limit strength destroying cementation, and the mass volume changes associated with vein production. If drainage is prevented or impeded, stress will develop in the pore water opposing the externally applied stress increase associated with crack propagation. Therefore, pore water pressures are a controlling factor on stability or local/global failure during construction. Measurement of movements and deformations is as important to assess internal damages as the measurement of pore pressures. Generally, piping must particularly be guarded against because it occurs gradually through seepage and is often not apparent until either crack path remediation or the structure’s failure is imminent. Seepage and erosion along the lines of vein, continuous crack or local poor compaction and through cracks in foundations and concrete mass may specially be indicated by such measurements.

In this research, numerical analysis of concrete dams are based on radical simplifications of the on plane stress or strain patterns defining internal mechanism and the shape of the rupture planes. However, accurate measurement of stress/strain/pore pressure is sometimes difficult and distribution of stress/strain in concrete dams is complex. Strains may be calculated either from displacements, mechanical constitutive equations or be measured directly which may not be conformed to due to several known or unknown reasons.

### 4. DAMAGE EFFECTS ON MODULUS MATRIX

The proposed damage model constitutive modulus matrix is computed from superposition of its counterparts on the multi-laminate that such counterparts in turn, are calculated based on the plasticity and damage occurred on each sampling plane during deformation depending on its specific loading conditions and crack growth [8,9]. The on plane dislocations are evaluated according to the combination of two proposed functions; each of them is due to strain exceeding the particular on plane damage limit. This two loading conditions are as follows:

**I. axial,  $w_{axial}$  :**  $w_{ax}(x(\epsilon_{ax})) = [1 - e^{-a_{ax} \times x(\epsilon_{ax})}] \cdot H(x(\epsilon_{ax}))$  (1-a)

**II. Shear,  $w_{shear}$  :**  $w_{sh}(x(\epsilon_{sh})) = [1 - e^{-a_{sh} \times x(\epsilon_{sh})}] \cdot H(x(\epsilon_{sh}))$  (1-b)

$a_{ax}$  and  $a_{sh}$  are two material constant,  $\epsilon_{ax}$  and  $\epsilon_{sh}$  are on plane axial and shear strain. Therefore, function  $x(\epsilon)$  is written as follows:

$$\epsilon_{ax} = \epsilon_N, \quad \epsilon_{sh} = \sqrt{\epsilon_M^2 + \epsilon_L^2}, \quad x(\epsilon) = (\epsilon - \epsilon_0) / \epsilon_0 \tag{2}$$

$\epsilon_0$  stands for starting damage dislocation strain. Also, Heaviside function is introduced as follows:

$$H(x(\epsilon)) = \begin{cases} 0 & : x(\epsilon) \leq 0 \\ 1 & : x(\epsilon) > 0 \end{cases} \tag{3}$$

The calculation of damage plane modulus matrix and on plane stress components are as follows:

$$\begin{Bmatrix} \sigma_{Ni} \\ \sigma_{Mi} \\ \sigma_{Li} \end{Bmatrix} = [D_i] \begin{Bmatrix} \epsilon_{Ni} \\ \epsilon_{Mi} \\ \epsilon_{Li} \end{Bmatrix}, \quad [D_i] = \begin{bmatrix} 1-w_{axial} & 0 & 0 \\ 0 & 1-w_{shear} & 0 \\ 0 & 0 & 1-w_{shear} \end{bmatrix} \begin{bmatrix} E_N & 0 & 0 \\ 0 & E_T & 0 \\ 0 & 0 & E_T \end{bmatrix}, \quad \begin{matrix} E_N = E / (1-2\theta) \\ E_T = E_N \cdot (1-4\theta) / (1+\theta) \end{matrix} \tag{4}$$

To transfer the on plane stress matrix (size: 3x1) to global coordinate (6x1) and summing them up upon numerical integration equation can be written as follows:

$$\sigma_{ij} = 6 \sum_{i=1}^{17} w_i [L_i]^T \{ \sigma_{Ni} \quad \sigma_{Mi} \quad \sigma_{Li} \}^T \tag{5}$$

$L_i^T$  is transformation matrix (3x6). The on plane compliance matrices (3x3) are found by the following equation to be summed up to obtain main compliance matrix C (6x6) as follows:

$$[C_i] = [D_i]^{-1} \quad [C] = 6 \sum_{i=1}^{17} w_i [L_i]^T [C_i] [L_i] \quad (6)$$

Also, the variation of strength due to damage can be obtained by two strength functions as follows:

$$R(x(\varepsilon_{eq})) = \begin{cases} c.e^{d.x(\varepsilon_{eq})} & x(\varepsilon_{eq}) \leq b \\ g.e^{f.x(\varepsilon_{eq})} & x(\varepsilon_{eq}) \geq b \end{cases}, \quad \varepsilon_{eq} = \sqrt{\varepsilon_N^2 + \varepsilon_M^2 + \varepsilon_L^2} \quad (7)$$

where  $b, c, d, f$  and  $g$  are material properties. The value of  $g$  is found upon continuity of function  $R(x(\varepsilon_{eq}))$  at the location  $x(\varepsilon_{eq}) = b$ .  $\varepsilon_{eq}$  is on plane equivalent strain. To ease the analogy of projections of stress and strain tensors on sampling planes, the behavior of material can be divided into two distinct parts as on plane normal (volumetric) and shear (deviatoric). Consequently, modulus matrix at the center of unit sphere is obtained by integration its variation over sphere surface. This integration can be calculated numerically through sampling points correspond to sampling planes. As a result, the point modulus matrix after some manipulations is written as follows:

$$D_{ijkl} = \frac{3}{4\pi} \int_{\Omega} \left( \frac{E}{1+\nu} \right) \left[ \left( N_{ij} - \frac{\delta_{ij}}{3} \right) \left( N_{kl} - \frac{\delta_{kl}}{3} \right) + M_{ij} M_{kl} + L_{ij} L_{kl} \right] d\Omega + \frac{E}{1-2\nu} \frac{\delta_{kl}}{3} \delta_{ij} \quad (8)$$

$M_{ij}, N_{ij}$  and  $L_{ij}$  are components of transformation matrix.

### 5. ON PLANE STRAIN EFFECTS ON PERMEABILITY

According to *Choinska et al. (2007-b)* [10], the general permeability changes versus the strain ratio defining damage function for different types of concrete has been presented as shown in Figure 3-a. The permeability ellipsoid is shown in Figure 3-b. A cracked sampling upon corresponding on plane strain ratio as a damaged plane makes a local jumped value on permeability ellipsoid of Gauss point to evaluate the crack effects of hydraulic conductivity. This local jump can be assumed belong to a new higher level similar permeability ellipsoid that its diameters multiplied by  $\sqrt{\omega}$  ( $\omega = \frac{k_{ni(new)}}{k_{ni}}$ ) that can be accounted as follows:

$$k_{ni(new)} = \frac{\sqrt{\omega} A \cdot \sqrt{\omega} B}{\sqrt{(\ell_i^2 + m_i^2)(\sqrt{\omega} A)^2 + n_i^2(\sqrt{\omega} B)^2}} = \sqrt{\omega} k_{ni} \quad (9)$$

With this regards, calculating the  $i^{th}$  plane strain ratio, damaged permeability matrix is provided and the new permeability matrix of  $i^{th}$  plane has been replaced to obtain the corresponding Gauss point permeability matrix in FEM solution. The strain components and damage function for 17 planes can be computed upon multi-laminate damage model, (Labibzadeh, M., Sadrnejad, S. A., 2006) [11, 12], Sadrnejad, S. A., et al., 2002 ) [13].

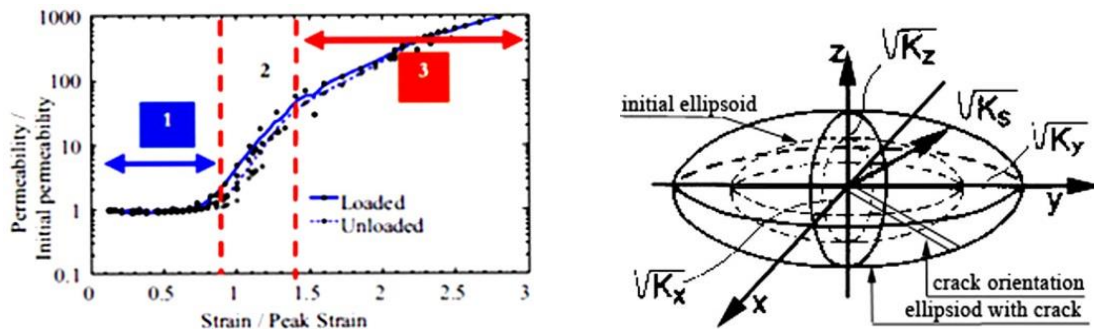


Figure 3 a) Permeability changes vs. the strain ratio [13], b) Initial, cracked affected ellipsoids

The governing equations for single phase flow and transport in a saturated aquifer are the continuity equation combined with Darcy's law as follows:

$$S_0 \frac{\partial h}{\partial t} + \text{div}[(8\pi \sum_{i=1}^n w_i T_i^T K_i^D T_i) \text{grad}(h)] = q \quad (10)$$

Therefore, the advection–dispersion transport–equation employed is as follows:

$$\frac{\partial c}{\partial t} + \text{div}(cv) - \text{div}[(8\pi \sum_{i=1}^n w_i T_i^T K_i^D T_i) \text{grad} c] = r \quad (11)$$

where  $S_0$  represents the specific storage coefficient,  $h$  the piezometric head,  $t$  the time,  $K_i^D$  the hydraulic conductivity tensor for  $i^{\text{th}}$  plane,  $c$  the solute concentration,  $v$  the seepage velocity,  $q$  flow flux,  $r$  externally applied source and sink terms,  $T_i$  is transformation matrix for  $i^{\text{th}}$  plane and  $n$  is number of sampling planes.

The permeability matrix  $K_i^D$  for  $i^{\text{th}}$  plane is a  $3 \times 3$  matrix in Cartesian coordinate built on  $i^{\text{th}}$  plane, including the effects of strain tensor variations of corresponding plane. The transformation matrix is defined for three perpendicular planes at global Cartesian coordinate of each Gauss points; therefore,  $T_i$  for each set of three planes corresponding to  $i^{\text{th}}$  plane. Summing up the permeability matrices of all sampling planes, a numerical integration rule and corresponding transformed weighted matrix of all planes must be employed as follows:

$$K_{Gauss}^D = 8\pi \sum_{i=1}^n w_i T_i^T K_i^D T_i \quad (12)$$

## 6. DAMAGE DETECTION METHOD

The existing safe condition solution of a concrete dam with a certain water level must be ready as initial conditions for any damage computation. A numerical analysis of current condition must be conducted to provide a complete evaluation of different current variables such as stress, strain, deformations, and excess pore water pressure as nonconformity or disorder in records. Therefore, any unexpected non-conformed values measured by right instrument reading presented through stress or strain meters, piezometer or other instruments is known as a signal for the occurrence of a damage. A difference vector as the net disorder values is defined by jump values with regards to initial normal values as lack of conformity components. These vector components must be converted to a loading vector composed of equivalent nodal forces that can be incrementally and carefully applied to nodes in vicinity of instrument sensors. The aim of this gradual numerical back analysis is to find any abnormal condition as on plane stress/strain disorders which may be created by satisfying gradually equilibrium, compatibility and on plane undamaged/damaged constitutive equations. The maximum care must be employed checking any condition that exceeds limitations or may break assumption of continuity through materials. Therefore, any sharp hydraulic gradient, quick seepage flows through the vein, stress component reductions, strain component increase or sever deformations effects on plane widening/closing/sliding lead to create heave as local void ratio increase, appearing veins and unexpected seepage, local different types of crack. Such a control can be numerically carried out up to local or even global failure that may happen.

## 7. RESULTS OF CRACKS IN SEFID-ROOD BUTTRESSED DAM

This dam height is 106 m. with 417 m. of crest length that was built in between 1956 to 1963 in Gilan state at north of Iran. The dam downstream view is shown in Figure 4-a. Due to earthquake magnitude 7.3 Richter 1990, rib base no.18 of this dam cracked and some seepage started at the shown located in Figure 4-b that later on, it was amended by resin injection. This rib base was modeled through FE developed computer program and the internal damages and permeability changes predicted. Figure 5-a and 5-b show the combined stress distribution before and after earthquake, respectively. The concrete mechanical properties are shown in Table 2.

**Table 2: Concrete properties**

Dynamic Young Modulus $E_d$ (MPa)	Elastic Young Modulus $E$ (MPa)	Poisson' ratio $\nu$	Density ( $kg/m^3$ )	Compressive strength $f'_c$ (MPa)
29000	20000	0.17	2250	16.9

The FE mapped mesh of rib number 18 including first cracked locations are shown in Figure 6. The first failed plane number 8 at node 85, as combined stress and normal strain time histories are presented in Figure 7-a and 7-b. The plane no. 8 of node 85 normal stress vs. strain and its time history and also its stress path plus the orientation of this failed plane are presented in Figure 8.

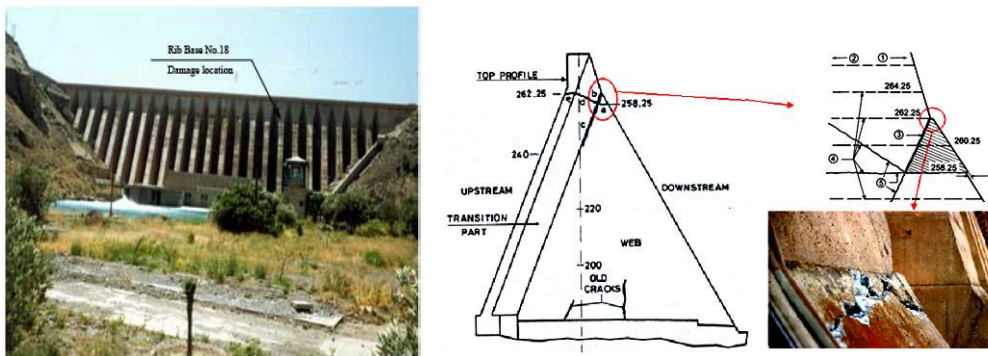


**Figure 4-a) Sefid-Rood dam down stream view, b) downstream cracks view of rib number 18 and cracks location**

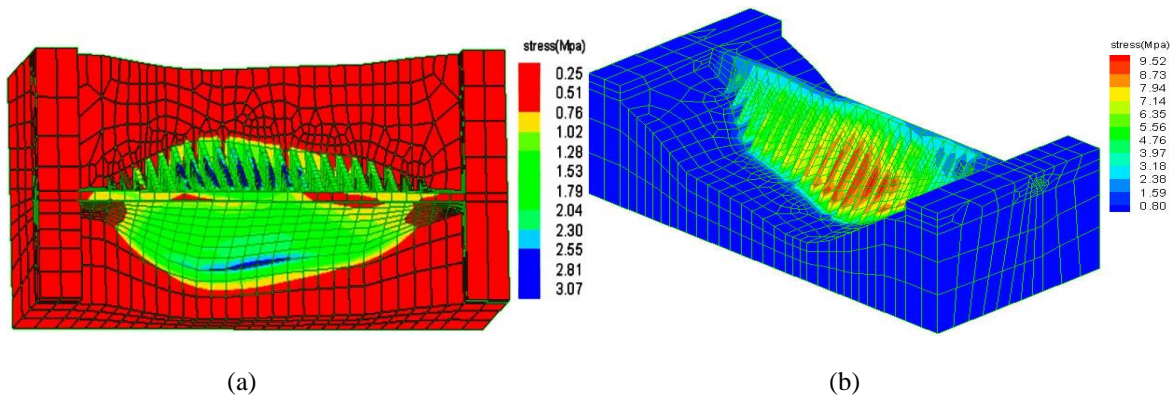


**Figure 5 Dam combined stress analysis, a) before and b) after earthquake**

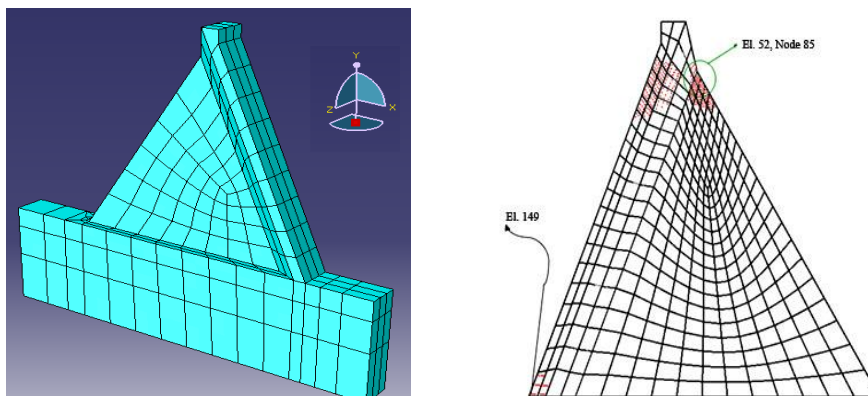


**Figure 6 a) Mapped elements and b) damaged locations**

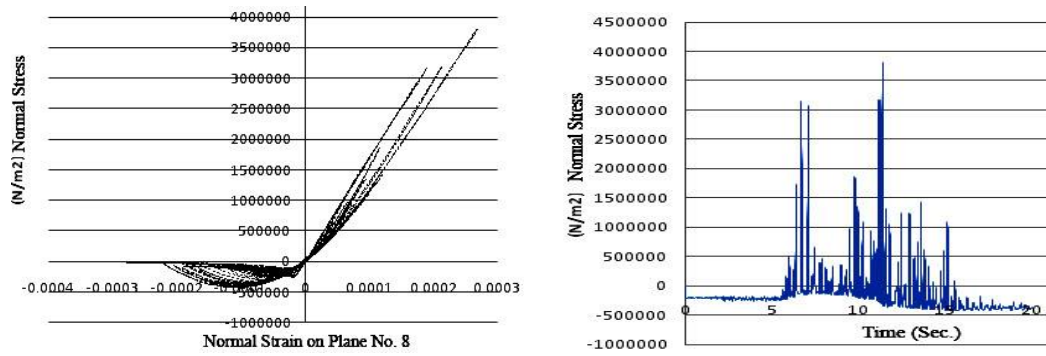


**Figure 7 a) normal stress vs. strain, b) time history of Normal stress on plane no. 8 of Node 85**

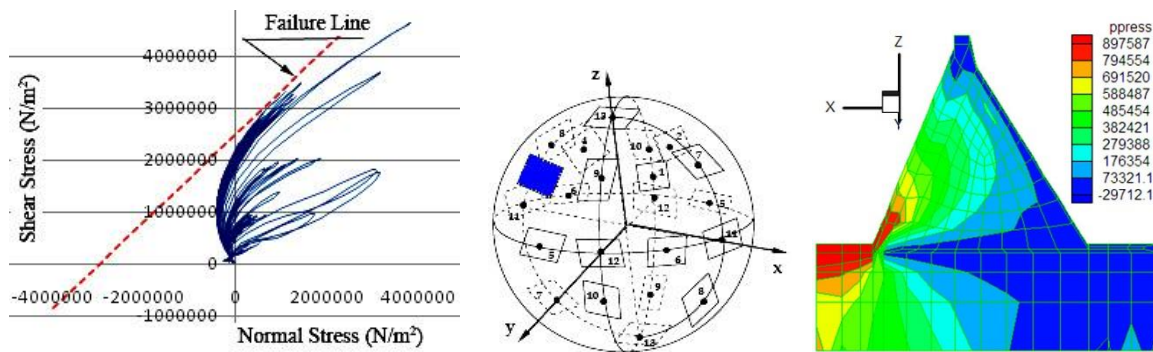


**Figure 8 a) stress path on plane no. 8, b) its direction on sphere, and c) initial P.W.P.**

Figure 9 show pore water pressure (P.W.P.) contours and the comparison of measured hydrostatic pore water pressure at the piezometer locations after 4 seconds since the start of earthquake with model results. To show the capability of proposed model, the two measured pore water pressure histories at piezometer no. 139 and 435 during earthquake are compared with model results in Figure 9-a and -b respectively. This comparison reveals that the proposed model is quite capable of predicting such a dynamic damage history after earthquake.

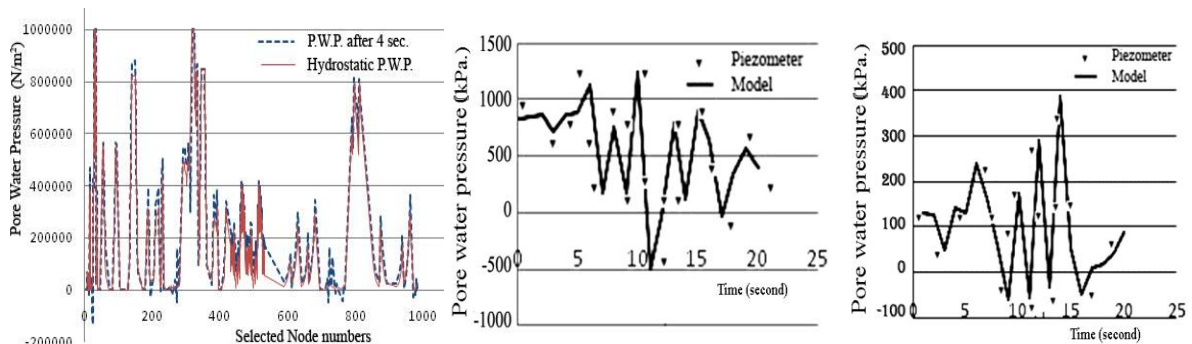


**Figure 9 a) comparing pore water pressure after 4 seconds with hydrostatic P.W.P., b) P.W.P. at piezometer No. 139 and 435 during earthquake**

## 8. CONCLUSIONS

A certain accurate program is required to record and data acquisition of any concrete structure instruments usage. Current trends in the field of instrumentation emphasize the search for higher resolution and precision, providing more accurate measurements and permitting rapid detection of any behavioral anomalies

through structure. A damage permeability tensor containing crack orientation effects associated with fracture generation in multi-laminate framework has been developed and employed to examine the influence of fracture–matrix interaction on flow and transport processes. The proposed model results on concrete dam have shown that, the presence of a fractured matrix in a fractured system leads to a considerable conductivity matrix change affecting pore water pressure, and the flow and transport conditions through a cracked concrete medium. A simple multi-laminate technique has been able to evaluate different damages as crack opening displacement/sliding and permeability tensor change based on orientation damage, led to failure mechanism analyses.

A certain flow gradient approach which is equivalent to a non-local average with a sharper distribution, lending less weight to neighboring points compared to the non-uniform Gaussian distribution in the classical integral approach. Therefore, this gradient approach provides better limit values of the quality for a formed crack than with the integral model.

In closing, it should be recalled that dam monitoring is a key component of dam safety. Because the failure of a dam can lead to human as well as economic disaster, no compromise in regards to instrumentation quality or reliability should be made.

## 9. REFERENCES

1. Christofferson, Mehrabadi M. M. and NematNasser, S., A micromechanical description of granular behavior, *J. Appl. Mech.*, 48, 339344 (1981),
2. NematNasser, S. and Mehrabadi M. M., Stress and fabric in granular masses, *Mechanics of granular Materials: New Models and Constitutive Relations* (Eds. J.T. Jenkins and M. Satake), pp. 18, Elsevier Sci. Pub., 1983.
3. Sadrnejad S. A., (1992) Multilaminar elastoplastic model for granular media. *International Journal of Engineering* 5: 11.
4. Sadrnejad S.A., Shakeri, S., (2017), Multi-laminate non-coaxial modelling of anisotropic sand behavior through damage formulation, *Computers and Geotechnics* 88 (2017) 18–31
5. Sadrnejad, S, A., Labibzadeh, M., "A *Continuum/ Discontinuum Micro Plane Damage Model for Concrete*", *International Journal of Civil Engineering*, Vol. 4, pp. 296-313, 2006.
6. Sadrnejad S.A., (2006), Numerical Evaluation of Non-homogeneity and Anisotropy due to Joints in Rock Media, *International Journal of Civil Engineering*. Vol.4, No. 2.
7. Sadrnejad S.A. and Karimpour H., (2011), Drained and Undrained Sand Behaviour by Multilaminar Bounding Surface Model, *International Journal of Civil Engineering*, vol.9, No.2
8. Sadrnejad S.A., Hoseinzadeh, H.R., (2017), Multi-Laminar Rate-Dependent Modelling of Static and Dynamic Concrete Behavior through Damage Formulation, *Scientia Iranica, Transaction A, Civil Engineering*, (accepted to be published).
9. Sadrnejad S.A., Multi-laminar elasto-plastic model for granular media, *Journal of Engineering, Islamic Republic of Iran*, vol.5, Nos.1&2, May 1992-11.
10. Choinska, M., Gilles Pijaudier-Cabot, Frédéric Dufour, 2007-b, Permeability due to the Increase of Damage in Concrete: From Diffuse to Localized Damage Distributions, *Journal of Engineering Mechanics* Sep 2009, Vol. 135, No. 9, pp. 1022-1028, Online Publication Date: 6 Mar 2009, [http://ascelibrary.org/doi/abs/10.1061/\(ASCE\)EM.1943-7889.0000016](http://ascelibrary.org/doi/abs/10.1061/(ASCE)EM.1943-7889.0000016)
11. LABIBZADEH, M., SADRNEJAD, S. A., Mesoscopic Damage Based Model for Plane Concrete under Static and Dynamic Loadings. *American Journal of Applied Sciences*, 3(9): 2011-2019, 2006.
12. LABIBZADEH, M., SADRNEJAD, S. A., Dynamic Solution Code for Structural Analysis upon Joint Element. *Journal of Computer Science*, 2(5): 401-409, 2006.
13. Sadrnejad S.A., "A *sub-loading surface multi-laminar model for elastic plastic porous media*", *IJE*, Vol. 15, No.4, Nov. 2002.